Biobased Films from Amphiphilic Lignin-Graft-PLGA Copolymer

Omar E. Mendez,[a] Carlos E. Astete,[a] Soňa Hermanová,[b] Dorin Boldor,[a] William Orts,[c] and Cristina M. Sabliov [a,*]

Amphiphilic copolymers were synthesized by grafting poly(lactic-co-glycolic) acid with two lignin types: alkaline lignin and lignosulfonate. An interphase formation technique was used to produce films based on the copolymers. Films presented one side as being more hydrophobic (O-side) and smoother, and the second side more polar and with an uneven surface (W-side). Contact angle of water on the W-side was lower than the O-side corresponding to a higher lignin content and influenced by the lignin type (alkaline < lignosulfonate) and lignin: PLGA ratio. X-ray photoelectric spectroscopy analysis showed higher percentages of sulfur on the W-side, which supports a preferential partitioning of the lignin. Tensile testing demonstrated the significant impact of lignin type on the mechanical properties of the films. Alkaline films showed a higher maximum strength, a higher stiffness, and a higher tensile strength at the elastic limit compared to lignosulfonate films. However, for lignosulfonate films, ductility at break point was 4-fold higher than that of alkaline films.

DOI: 10.15376/biores.18.3.5887-5907

Keywords: Lignin; Biodegradable films; Amphiphilic; Contact angle; X-ray photoelectric spectroscopy

Contact information: a: Biological & Agricultural Engineering, Louisiana State University and LSU Ag Center, Baton Rouge, LA, USA; b: Faculty of AgriSciences, Mendel University in Brno, Brno, Czechia; c: USDA, Agricultural Research Service, Western Regional Research Center, Beltsville, MD, USA;
** Corresponding author: csabliov@lsu.edu*

INTRODUCTION

To overcome the environmental problem caused by resistant plastics, waste, and microplastics residues, and to increase sustainability of agricultural crop production, packaging films made from biodegradable polymers and biopolymers from renewable resources degrading into carbon dioxide (biogas under anerobic conditions) and water are proposed as a viable solution (Menossi *et al.* 2021).

In addition to polysaccharide biocomposites, lignin (LN) was studied as a suitable material for sustainable packaging application (Zadeh *et al.* 2018). LN, a biopolymer abundantly available as waste product in the pulping refinery process, possesses UV absorption and antioxidant properties, high thermal stability, and adhesivity. Due to various functional groups in its structure, LN can interact with synthetic polymers forming chemical products with novel unique properties (Alzagameem *et al.* 2022).

LN with different structures and degrees of purity can be produced depending on the process utilized, primarily base or acid catalyzed mechanisms; alkaline lignin (ALN), and lignosulfonates (SLN) (Vásquez-Garay *et al.* 2021). The sulfite process is used in pulping processes; it is an acid-catalyzed mechanism that involves the cleavage of the α-

ether linkages and β-ether linkages of LN that results in SLN. ALN and SLN are both extracted from the pulping process. ALN is produced during the kraft pulping process; it is dissolved into black liquor and is less soluble in water than SLN, but it is soluble in alkali solutions because of the high concentrations of hydroxyl groups (Ganawatta *et al.* 2019). The ALN is processed using mixtures of NaOH and Na_2S at pH 13. Meanwhile, SLN is produced using an aqueous solution of (SO_2) at pH 1 or 2 (Laurichesse and Avérous 2014). Because of the higher amount of sulfonate groups in SLN, it is typically more water-soluble. SLN also has a higher average molar mass (15000 to 50000 g mol^{-1}) than ALN (1000 to 3000 g mol^{-1}) (Lu and Ralph 2010).

In contrast, polylactic acid (PLA)/LN composite polymers have been developed and shown to improve the gas barrier performance in food packaging (Wang *et al*. 2020). The addition of LN to a polylactic acid-graft-glycidyl methacrylate (PLA-g-GMA) polymer resulted in an increase of 33% in the tensile strength of the films. Similarly, UV-absorbent lignocellulosic butanol graft copolymer was developed with superior UV-protective capacity. The copolymer could absorb 96.2% of UV irradiation in the range of 200 to 315 nm (Liu *et al.* 2014).

To the best of the authors' knowledge, amphiphilic films made from LN grafted with poly(lactic-co-glycolic) acid (PLGA) have not been studied to this date. The objective of this study was to investigate the effect of LN treatment (ALN vs SLN) on the physical-chemical and mechanical performance of LN-graft-PLGA films. Copolymers were synthesized using a ALN and SLN at different ratios relative to PLGA (1:4 and 1:6 w/w LN:PLGA), and films were produced from the (A/S)LN-g-PLGA polymers with an interphase forming process at 0, 5, and 20% glycerol. Lignin, with a high number of -OH and -SH groups in its structure, has a high affinity for water (Lu and Ralph 2010), whereas PLGA with its methyl groups is more hydrophobic (Lu and Ralph 2010). Thus, the hypothesis was that because of the different solubility of LN and PLGA in water, the polymer film would arrange itself such as the hydrophilic groups of LN segment will be facing towards the water phase (W-phase), and the more hydrophobic PLGA segment towards the organic phase (O-phase). The physical, chemical, and mechanical characteristics of the (A/S)LN-g-PLGA films were determined by scanning electron microscopy (SEM), contact angle measurements, X-ray photoelectric spectroscopy (XPS) analysis, and tensile test analysis.

EXPERIMENTAL

Materials

Alkaline lignin (ALN) and sodium lignosulfonate (SLN) were purchased from TCI (Portland, OR). Oxalyl chloride, dimethylformamide (DMF), ethyl acetate, and dimethyl sulfoxide (DMSO) were obtained from Fisher Scientific (Fair Lawn, NJ). Dichloromethane (DCM) was purchased from Supelco (Burlington, MA), and poly lactic-co-glycolic acid (PLGA) was acquired from Sigma Aldrich (St. Luis, MO). Deionized (DI) water was obtained by using a Barnstead Smart2Pure water purification system (Barnstead International, Dubuque, IA).

Polymer Synthesis

The grafting process of PLGA on LN to form LN-g-PLGA polymer was achieved *via* an acylation reaction. An amount of 4 g of PLGA was placed in a three-neck bottom flask and dissolved in 100 mL of dichloromethane (DCM) at room temperature. When the PLGA was fully dissolved, 100 µL of oxalyl chloride was added dropwise with a glass syringe and 4 mL of dimethylformamide (DMF) were added as a catalyst. The mixture was stirred for 5 h to synthesize PLGA-Cl. The PLGA-Cl was concentrated in a Buchi R-300 rotavapor (Buchi Corporation, New Castle, DE, USA). Next, 30 mL of dimethyl sulfoxide (DMSO) containing LN were added to the PLGA-Cl solution. The amount of LN dissolved in the 30 mL of DMSO was 1 or 0.67 g for the 1:4 and 1:6 w/w LN:PLGA ratios, respectively. The LN and PLGA-Cl solution were mixed overnight under nitrogen flow. The LN-g-PLGA polymer was precipitated in 200 mL of ethyl ether and washed three times in ethyl ether to remove the remaining DMSO from the polymer. The LN-g-PLGA polymer was dissolved in 40 mL of DCM and washed with water in a decantation flask three times to remove traces of unreacted LN. The LN-g-PLGA polymer was concentrated in a rotavapor Buchi R-300 (Buchi Corporation, New Castle, DE, USA) and freeze-dried using Labconco Free zone 2.5 plus (Labconco, Kansas City, MO, USA).

Film Formation

The polymeric films were made from the graft polymer using the interphase forming process (Santos *et al.* 2019). The LN-g-PLGA (200 mg) was dissolved in 10 mL ethyl acetate at a concentration of 2.0% (w/v). The solution was mildly stirred for 30 min and sonicated for 5 min in a Branson 3510 sonicator bath (Branson Ultrasonics Corporation, Danbury, CT, USA). After solubilization, glycerol was added as a plasticizer (0, 5, and 20% w/w) and stirred for 30 min. The solution was poured in beakers with 40 mL of water saturated with 8 mL of ethyl acetate and left for three days under a hood for the organic solvent to evaporate. Finally, the resulting films on the water surface (Fig. SI) were stored in a desiccator at room temperature with a saturated magnesium chloride solution to keep relative humidity at 34%. The formed films had a hydrophobic side (O-side) facing the organic solvent, and a hydrophilic side (W-side), facing the water phase.

Experimental Design

LN-g-PLGA films were made from ALN and SLN using two different ratios of LN to PLGA (1:4 and 1:6 w/w LN:PLGA), and with PLGA alone as a control. Glycerol was used as a plasticizer in three concentrations (0%, 5%, and 20% w/w) with the 0% being a control treatment (Table 1).

Table 1. Experimental Design

Polymer	LN:PLGA Ratio (w/w)	Glycerol (%)		
PLGA (Control)	N/A	0	5	20
ALN-g-PLGA	1:4			
	1:6			
SLN-g-PLGA	1:4			
	1:6			

Scanning Electron Microscopy

Morphology of the films was assessed using SEM. Samples were coated with Platinum (Pt) to avoid the effect of charging during analysis and were fixed in a double-sided carbon type tape. The SEM images were acquired using a FEI Quanta 3D FEG dual-beam FIB/SEM microscope (FEI/Thermo Fisher, Waltham, MA, USA) and detected with EDAX Apollo XL EDS detector (EDAX/AMETEK, Mahwah, NJ, USA).

Contact Angle

The hydrophobicity of the films was assessed by a sessile drop test measuring the contact angle with an optical tensiometer Attention Theta (Biolin Scientific, Beijing, China). Droplets (15 µL) of deionized (DI) water were placed on each side of the films (O and W) and the contact angle was measured at 30 seconds.

XPS Analysis

Chemical composition analysis was completed using XPS analysis as follows. Samples were cut into 1 × 1 cm^2 pieces and fixed into a double-sided carbon tape. Samples were arranged such as either the O or the W side faced upwards to analyze both sides. The samples were loaded and degassed in vacuum (5×10^{-7} mBar) for 4 h before analysis. The XPS measurements were performed using a ScientaOmicron ESCA 2SR X-ray photoelectron spectroscope system (ScientaOmicron, Taunusstein, Germany) equipped with a flood source charge neutralizer. A wide region survey scan was performed for each sample, followed by a high resolution scan for Carbon (C) and Sulfur (S). All elements were calibrated with the C1s = 284.8 ev as a reference peak. Results were analyzed and processed using the CasaXPS program. The elements quantified were Sodium (Na), Oxygen (O), Carbon (C), Chloride (Cl), Sulfur (S), Silicon (Si), Fluorine (F), Calcium (Ca), Nitrogen (N), and Tin (Sn) for a total of 100%. Different carbon bonds were quantified as percentage adding up to 100%.

Shrinking of Polymer Films

Films were cast in 100-mL beakers and had an initial area of 15.9 cm^2. Films were initially wet when extracted. After drying for three days under the hood, the area of the films was measured. A shrinking percentage was calculated based on the initial and final area of the films, as described in Eq. 1:

$$Shrinkage\ (\%) = 1 - \frac{Initial\ area\ (cm^2) - Final\ area\ (cm^2)}{Initial\ area\ (cm^2)} \quad (1)$$

Tensile Strength

Mechanical properties were measured by universal testing system series 5969 (INSTRON, Norwood, MA, USA). A tensile test was performed with a constant head speed of 15 mm/min. The maximum tensile strength, strength at elastic limit, rupture strength, maximum strain before break point, and Young's modulus were determined. Polymer films were cut into strips of approximately 12 × 25 mm^2. The width, length, and thickness of the polymer strips were measured using a micrometer (Anytime Tools, Los Angeles, CA, USA). Tensile strength and strain were measured from the tensile strength curve.

Statistical Analysis

The chemical and mechanical properties were analyzed with two and three-way analyses of variance (ANOVA), and multiple one-way ANOVA Tukey test in GraphPad Prism 9.3.1 (San Diego, CA, USA) with polymer type (ALN and SLN), LN to PLGA ratio (1:4 and 1:6 w/w), film side (W and O), and glycerol concentration (0, 5, and 20%). Significant difference was declared at $P < 0.05$.

RESULTS

Elemental Composition of Films

Elemental analysis for carbon (C), sulfur (S), and different bonds (C-C/C-H, C-O-C/C-OH, and C=O-C) was performed by XPS. Carbon was the most abundant element found in all films, at 64.97 ± 4.2% on average (Fig. 1 A). Statistical analysis showed no significant differences between carbon content for different LN types or the LN:PLGA ratio (Table S1); however, the surfaces of film sides showed a significant difference in the carbon content (P value = 0.0356). Higher differences were observed between the O-side and W-side of the ALN films compared to the SLN films (Fig. 1 A). This was reflected by the statistical analysis in which the interactions between the LN type and the side of the films showed a highly significant effect (P value = 0.0077), suggesting that the LN influenced the carbon content within the different sides of the films determining which side of the films would accumulate more carbon as expected based on the partitioning of the grafted films.

Films showed an average sulfur content of 0.7 ± 0.28 % for ALN films and 1.08 ± 0.94% for SLN films, both higher than PLGA control films (0.11 ± 0.16 %). This was expected, given the sulfur presence in LN but not in PLGA. W- side of the films had a significantly higher sulfur percentage (0.85 to 2.33%) compared to that of O-side of the films (0.22 to 0.54%) with P value = 0.002 (Fig. 1 B), further supporting the presence of LN on the more hydrophilic side of the film.

A significant difference (P value = 0.0462) was shown for the effect of LN to PLGA ratio (1:4 *vs*. 1:6 w/w) on the amount of sulfur detected. SLN films presented a more pronounced difference between sides at different LN:PLGA ratios with 2.33 ± 0.84, and 0.54 ± 0.17% for the W and O sides at 1:4 w/w ratio and 1.25 ± 0.14, and 0.22 ± 0.38% for the 1:6 w/w ratio. The LN type did not present a significant effect on the sulfur content of the films, but the P value = 0.0582 suggests that the effect of the LN should not be completely dismissed and should be considered further on (Table S1). This is further supported by the significance of the interaction between the LN type and the ratio of LN:PLGA obtained in the statistical analysis showing that the LN type had an effect on how the ratio affected the sulfur content of the films.

The films were analyzed by comparing the prevalence of different bonds: C-C/C-H, C-O-C/C-OH, and C=O-C (Fig. 1). The most abundant type of carbon bonds were determined as the C-C and C-H bonds, with an average of 52.55 ± 8.93%. The LN type showed an influence on the C-C/C-H concentration of the films, where ALN films had a higher C-C/C-H percentage than SLN films (Fig. 1 C). In contrast, ratio and LN types did not have a significant effect on the percentage of C-O-C and C-OH bonds, which were the second most abundant bonds measured with an average 31.59 ± 7.19%. Nevertheless, the processing history of the film side had a significant impact on the C-O-C and C-OH

percentage (P value = 0.0121). It can be seen (in Fig. 1D) that the percentage of C-O-C and C-OH on the O-side of the films was smaller than that of W-side.

Out of the carbon bonds, O-C=O showed the most differences across different films (Fig. 1 E). The ANOVA results indicated that the LN type had the highest significance regarding the percentage of O-C=O bonds found in the films (P value < 0.0001). PLGA showed the highest ester concentrations relative to the other films with 24.08 ± 5.9 and 28.08 ± 5.9% in the W and O sides, respectively. Nevertheless, the LN:PLGA ration of the films did not show an influence in the ester concentration of the films. Statistical analysis results also indicated that the interaction between the side, LN type, and ratio also had a significant effect on the percentage of the ester groups (Table S1). This would suggest that even though the ratio did not show an effect itself, it did affect how the ester groups were distributed in both sides of the films along with the LN type.

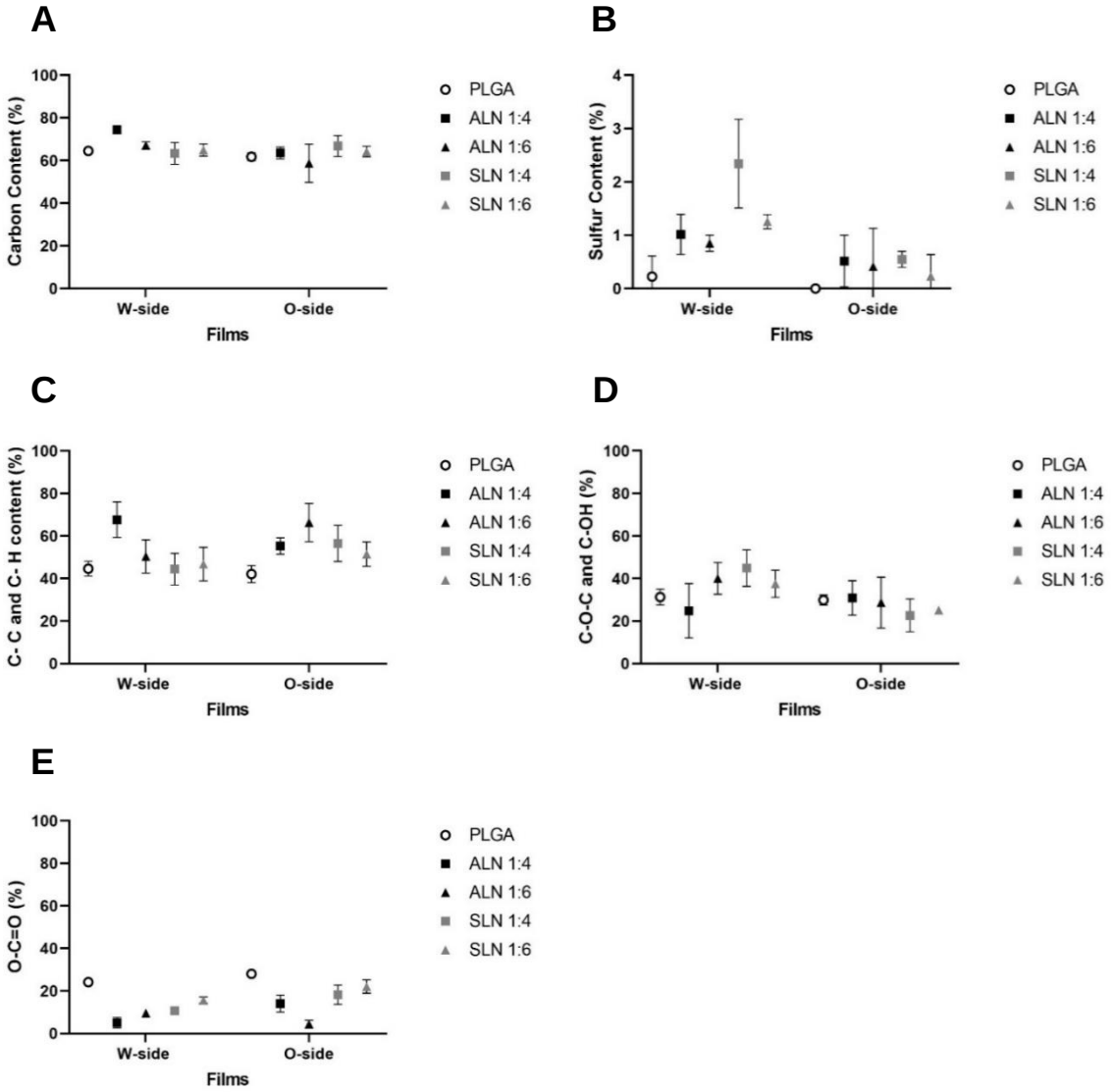

Fig. 1. XPS analysis for carbon, sulfur, and carbon bonds in (A/S)LN-g-PLGA films for both the W- and O- sides of the films made at 1:4 and 1:6 w/w LN:PLGA ratio and PLGA as a control: (A) Carbon content (%), (B) sulfur content (%), (C) C-C and C-H bonds, (D) C-O-C and C-OH bonds, and (E) O-C=O bonds; (n = 3)

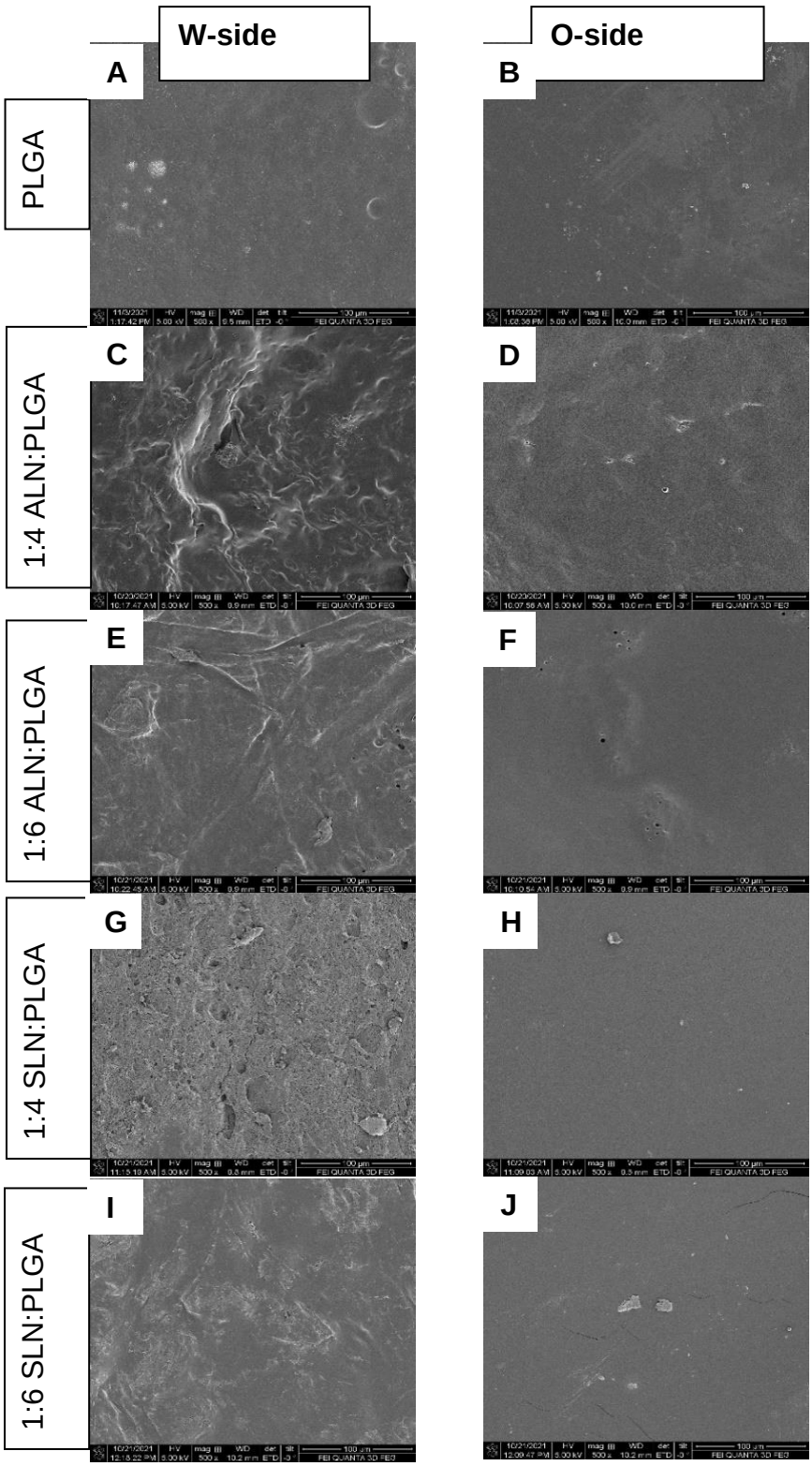

Fig. 2. SEM images for PLGA and (A/S)LN-g-PLGA films W-side (W), and O-side (O) made at different (A/S)LN:PLGA ratios: (A) PLGA W, (B) PLGA O, (C) ALN:PLGA (1:4 w/w) W, (D) ALN:PLGA (1:4 w/w) O, (E) ALN:PLGA (1:6 w/w) W, (F) ALN:PLGA (1:6 w/w) O, (G) SLN:PLGA (1:4 w/w) W, (H) SLN:PLGA (1:4 w/w) O, (I) SLN:PLGA (1:6 w/w) W, (J) SLN:PLGA (1:6 w/w) O

Surface Morphology and Hydrophobicity of Films

Morphology of the films was assessed using SEM. The PLGA films displayed similar character of both sides' surfaces (Fig. 2A, B). For all LN-g-PLGA films, O-side surface was smooth and approaching that of control PLGA film.

The W-side surface of all (A/S)LN-g-PLGA films was more irregular (Fig. 2C, E, G, and I) compared to the O-side surface of the films (Fig. 2D, F, H, and J) evidencing that the presence of LN affected the topological patterns. This is supported by more irregularities on the surface of W-sides for films with increased content of LN in copolymeric LN:PLGA 1:4 w/w materials (Fig. 2C, G) compared to LN:PLGA 1:6 w/w (Fig. 2E, I).

The LN influenced the morphology of the films; the less LN, the higher similarity between the morphology of the O-side surface of the LN-g-PLGA films to that of PLGA films.

Contact angle analysis was performed to determine the hydrophobicity of the film surface on both sides. The W-side of the films showed a lower contact angle overall compared to the O-side of the films (Fig. 3). The lowest values of contact angle were displayed by the ALN 1:4 w/w on the surface of W- side, measuring 27.2 ± 7.2°, 22.4 ± 7.5°, and 31 ± 4.8° at 0, 5, and 20% w/w glycerol respectively. The LN to PLGA ratios influenced the contact angle of the films; 1:4 w/w ratio films had lower contact angle compared to 1:6 w/w ratio on the W-side of the films for both ALN and SLN films.

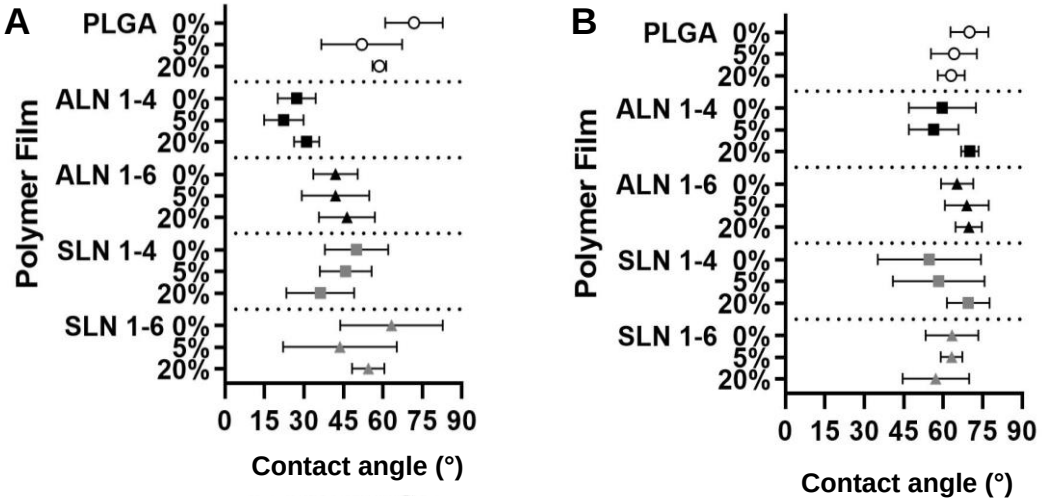

Fig. 3. Contact angle of (A) W- side, (B) O-side of the PLGA films (control) and (A/S)LN-g-PLGA films made at different (A/S)LN:PLGA w/w ratios, 1:4 and 1:6 w/w, and different plasticizer concentrations of 0, 5, and 10%; (n = 5)

Three-way ANOVA analysis was performed on each of the sides individually. The sources of variation measured were LN type, LN:PLGA ratio, and glycerol concentration. The LN type and LN:PLGA ratio were significant sources of variation only in the W-side of the films, with P-values of 0.0004 and 0.0006, respectively. Glycerol was not a significant source of variation in neither of the two sides (Table S2).

The effect of LN type, LN:PLGA ratio, and sides of the film were tested individually as well, using three-way ANOVA for each glycerol percentage. At 0% glycerol concentration, the side of the film, the LN type, and the LN:PLGA ratio all had a

significant effect on the contact angle values. At 5%, the side and the ratio of the films had an effect, while the LN type did not have an effect. At 20% glycerol concentration the only significant difference was found between the two sides of the films. These results suggested that at all glycerol concentrations the two sides of the films were very different, regardless of the type of LN used and the LN:PLGA ratio (Table S3).

Shrinking of Polymer Films

Tukey test showed that SLN films showed generally the highest difference in size when dried (Table S4), with a shrinking percentage of 49 and 44% for SLN 1:4 and 1:6 w/w, respectively. (Fig. 4).

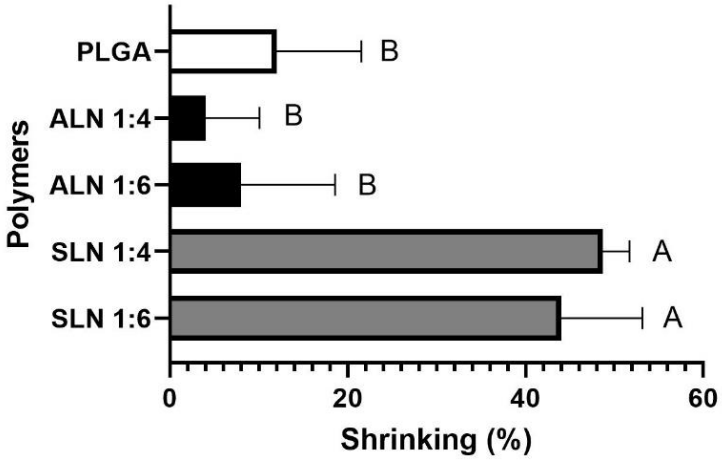

Fig. 4. Shrinking of polymer films (%) for ALN-g-PLGA and SLN-g-PLGA at two different LN:PLGA ratios (1:4 and 1:6 w/w) and PLGA as a control; (n = 3)

Thickness

The average thickness of the LN-g-PLGA films was 141 ± 35 µm overall, while the control PLGA films measured 116 ± 47 µm.

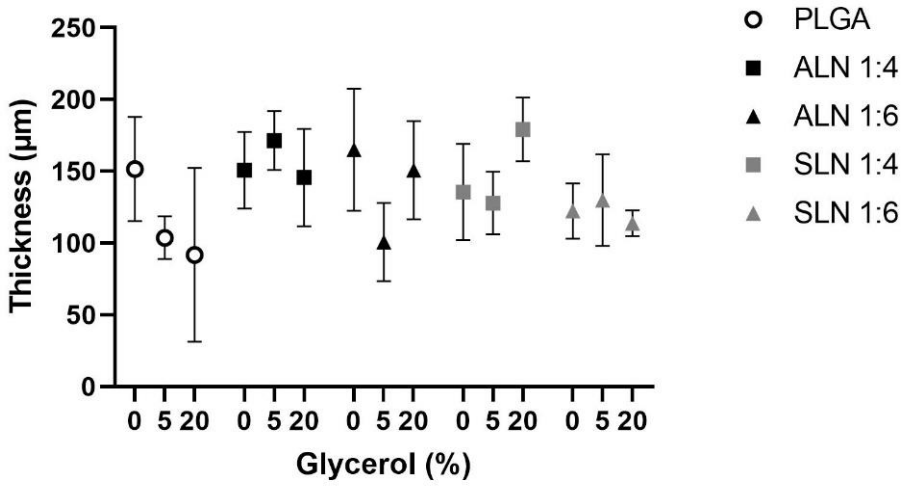

Fig. 5. Thickness of polymer films (µm) for (A/S)LN-g-PLGA at two different LN:PLGA ratios (1:4 and 1:6 w/w), three glycerol concentrations (0, 5, and 10%), and PLGA as a control; (n = 3)

Statistical analysis showed that films with a 1:4 w/w LN:PLGA ratios were significantly thicker than 1:6 w/w (Table S5). Average thickness for ALN and SLN 1:4 w/w films were 156 ± 28, and 147 ± 34 µm, respectively. In comparison, at 1:6 w/w LN:PLGA, ALN and SLN films were 139 ± 44, and 122 ± 22 µm thick (Fig. 5). These results demonstrated that even though the thickness of the films was not affected by the type of LN or percentage of plasticizer used, the LN:PLGA ratio had a significant effect.

Mechanical Properties

The maximum tensile strength (MPa), strength at elastic limit (MPa), rupture strength (MPa), strain to break point (%), and Young's modulus (GPa) were determined. The ANOVA analysis showed that the LN type was the main source of variation to the maximum tensile strength of the films ($P < 0.0001$) (Table S6). ALN films showed a higher maximum tensile strength compared to SLN films (Fig. 6 A) (13.51 ± 1.75 to 15.76 ± 3.94 MPa for 1:4 w/w films). Control films (PLGA) in comparison showed a maximum tensile strength similar to ALN films. This suggested that the presence of LN either strengthened (ALN) or weakened (SLN) the films.

Strength at the elastic limit was measured to determine the maximum strength applicable before permanent deformation. Statistical analysis showed that LN type had the highest significance in the strength of the films with a significance of $P < 0.0001$ (Table S6). Strength was higher in ALN films for ALN 1:4 w/w ratio at 0, 5, and 20% glycerol concentration compared to SLN films. The glycerol concentrations and the LN:PLGA ratio did not show an effect on the elastic limit strength (Fig. 6B).

ALN films showed a higher rupture strength compared to SLN films (Fig. 6C) (Table S6). In contrast, SLN films showed significantly lower rupture tensile strength compared to ALN films. PLGA films in comparison showed a rupture strength between ALN and SLN films. (Fig. 6 C).

The ductility of the films was measured by the total strain of the films before their breaking point. The strain of the films showed similar results as the tensile strength in the sense that the LN type was the main source of variation between films. In contrast to tensile strength, for strain, SLN showed a significantly higher strain in comparison to ALN films ($P < 0.0001$) (Table S6). (Fig. 6 D).

Finally, Young's modulus was used to determine the resistance of a material to deformation within the elastic region. The modulus was significantly influenced by both the LN type ($P < 0.0001$) and the LN:PLGA ratio ($P = 0.0115$), but not by the glycerol concentration (Table S6).

The highest Young's modulus was shown by ALN films and within ALN films, ALN 1:4 w/w had a lower modulus of elasticity and for SLN films ratio was important (Fig. 6E). The PLGA films showed a modulus in-between that of ALN and SLN films suggesting that even though the presence of PLGA influenced the stiffness of the films the main source of variation was the LN type used (Fig. 6E).

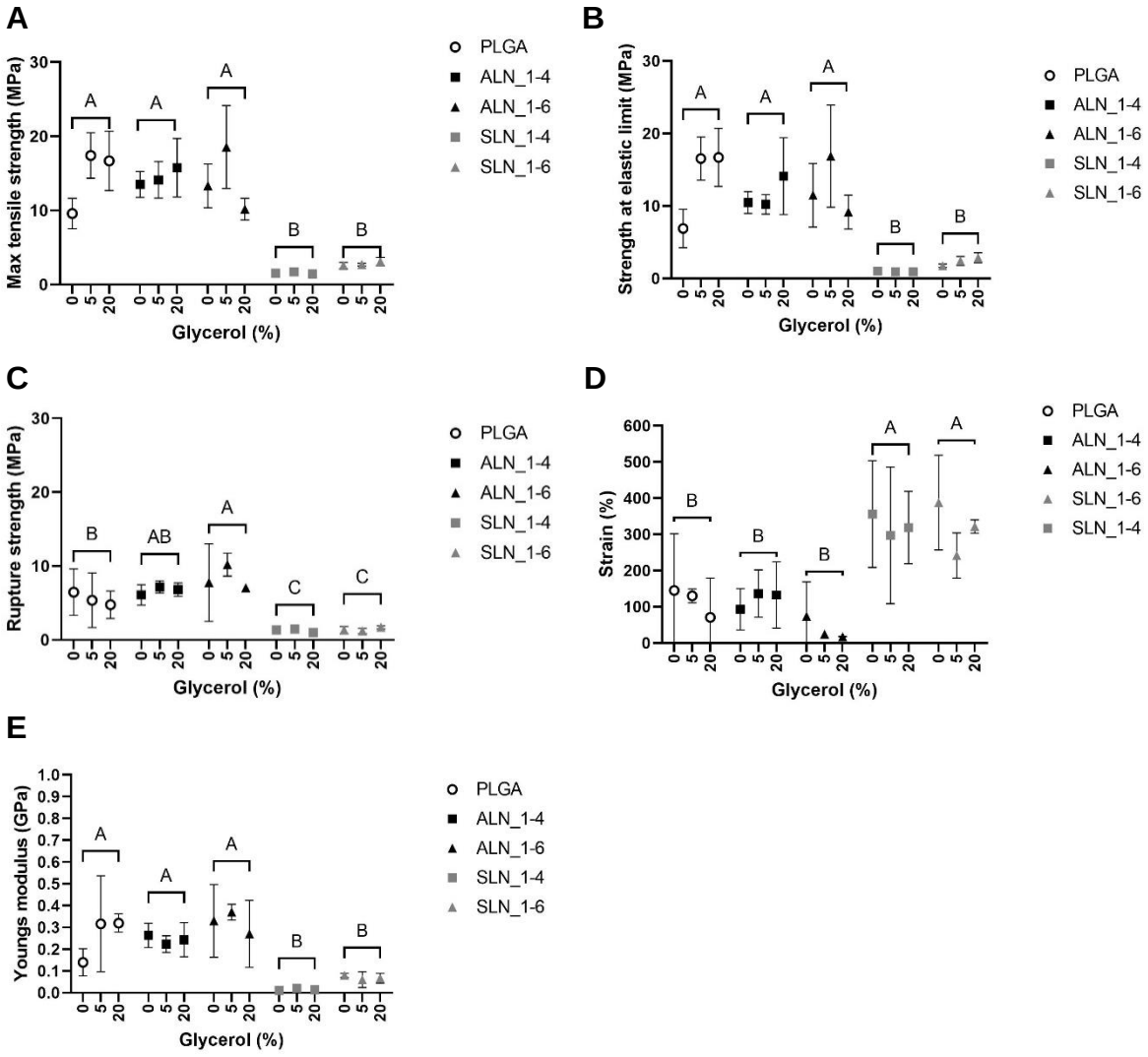

Fig. 6. Mechanical analysis for LN-g-PLGA films with two lignin types (ALN and SLN) and two LN:PLGA ratios (1:4 and 1:6 w/w): (A) Maximum tensile strength (MPa), (B) Tensile strength at the elastic limit (MPa), (C) Rupture tensile strength (MPa), (D) Ductility (mm/mm), (E) Young's modulus (GPa); (n = 3)

DISCUSSION

This study aimed to develop films having both hydrophilic and hydrophobic sides and to understand the effect of LN type on the properties of synthesized amphiphilic hybrid LN-based copolymers. Four types of amphiphilic copolymers were synthesized varying in LN types (ALN, SLN) and mass ratio (A/S)LN:PLGA = 1:4 and 1:6 w/w). The resulting graft copolymers were exposed at the interphase between an organic phase (O-phase =ethyl acetate) and an aqueous phase (W-phase = water) to form the films with O-side and W-side after solvent evaporation.

Elemental analysis was performed to evaluate the surface chemistry of O- and W-sides. C-C and C-H bonds were the most common in all films and are the most common in

organic molecules such as LN and PLGA. Higher O-C=O concentrations were determined on the O-side surface. Moreover, methyl groups (C-C and C-H) were slightly more abundant on the O- side of the films, even though the difference between the sides was only 2.17%. The difference of these bonds could be attributed to a higher distribution of PLGA segments on the O-side surface of the film.

Regarding hydroxyl (C-O-C and C-OH) functional groups, the results demonstrated that higher concentrations were found in the W-side of the films, which indicates preferential distribution of LN segments having hydroxyl groups as inherent part of the phenolic rings and aliphatic hydroxyl groups of LN (Huang *et al*. 2019). This was confirmed also by a higher sulfur content found in the W-side.

To observe the surface morphology, SEM analysis was performed. The SEM images clearly show differences between the O- and W-side with the W side of the films visibly more uneven and with irregularities than the O-side (Fig. 2). Contact angle results showed that there was a significant difference between the W- and O-sides of the films for all (A/S)LN:PLGA films, with W-side being more hydrophilic (lower contact angle) than O-sides (higher contact angle), while the PLGA control films presented similar contact angles on both sides (Fig. 3). Statistical analysis showed that the differences between LN types and LN:PLGA ratio were only significantly different on the W- side of the films but not the O-type of the films (Table S2).

The contact angle results for the two LN types indicated that the chemical composition of the LN-g-PLGA polymers was a relevant component of the hydrophobicity. SLN have a highly condensed structure and -SO_3 groups making it more soluble in water than ALN. Overall, SLN films had lower contact angle and higher wettability relative to ALN on the W-side of the films. Because -SH and -SO_3 groups are present in LN and not PLGA, the higher content of sulfur of the films also suggests a preferential spatial distribution of LN segments on the W-side and a higher affinity to water (Fig. 1 B). This could also explain the differences in thickness found between the different LN:PLGA ratios of the films. Because films with a higher LN content (1:4 w/w) ratio were thicker than films with less LN (1:6 w/w), it was suggested that LN may help to retain more moisture even after the drying of the films (Fig. 5). SLN:PLGA films showed more shrinking after the drying process, suggesting that SLN:PLGA films retained more water during the casting process and suffered a more severe shrinking effect after drying (Fig. 4). These findings are likewise related to those obtained with the contact angle analysis showing that SLN films had a stronger water affinity.

Mechanical properties of films were determined based on the initial stress/strain data. Among the mechanical characteristics, LN type was the main source of variation. ALN films showed a higher total and elastic limit tensile strength than PLGA and SLN films. Nevertheless, SLN films were able to extend more than ALN and PLGA films. Young's modulus was also lower in SLN films indicating that less stress was required to cause deformation. These results are supported by previously published studies that investigated the effect of LN on film properties. For example, addition of ALN and SLN to soy protein isolate films was reported to increase the films tensile strength by 230% for 10% ALN, and 170% for 10% SLN, respectively, compared to the control sample. Consequently, the addition of LN decreased the elongation of the films from 126 % (control) to 7.45%, and 79.95% after the addition of 10% ALN and SLN respectively (Zadeh *et al.* 2018). In agar films (Shankar *et al.* 2015) ALN addition also resulted in an increase in tensile strength with amounts as small as 3% w/w LN compared to neat agar

films. In a similar manner, plasticizing effects have been obtained in gluten matrices, in which the ductility of wheat-gluten increased from 120% to 250% with the addition of 20% SLN (Duval *et al.* 2013). Thus, it has been repeatedly demonstrated that the addition of LN can increase the tensile strength of polymer matrices. ALN in particular shows a higher capability to increase strength compared to SLN. Meanwhile, SLN is able to achieve a higher ductility compared to ALN. Mechanical properties of polymers can be dependent on the secondary bonds that chains generate between themselves or with water. The higher strain obtained in SLN films could be attributed to the presence of hydrogen bonds between the polymer and water and their plasticizing effect (Livi *et al.* 2015). This would correlate with the lower contact angle showed by SLN films, the higher shrinking percentage, and higher concentration of hydroxyl groups. In polymers, the arrangement of the polymer and entanglement have an effect in the mechanical properties as well as the thermoplastic properties.

CONCLUSIONS

1. Amphiphilic lignin-graft-poly(lactic-co-glycolic) acid (LN-g-PLGA) films were formed and showed different properties depending on the type of LN, LN:PLGA ratio, and glycerol.
2. The properties of the films were different across their water- and oil- sides (W-, and O-side). Contact angle, morphology, and chemical composition were different across sides.
3. LN type had a significant effect on the mechanical properties of the films. Alkaline lignin (ALN) had a higher maximum tensile strength and elastic limit strength.
4. Lignosulfonate (SLN) films showed a higher ductility shown by the higher extension percentage at break point. ALN films showed a higher Young's modulus compared to SLN films.
5. The differences between the W- and O- sides could be attributed to the chemical composition of the films as confirmed by X-ray photoelectron spectrometry (XPS) analysis, and the surface morphology measured by scanning electron microscopy (SEM).

ACKNOWLEDGEMENTS

This work was supported by the National Science Foundation under NSF EPSCoR Track 2 RII, OIA 1632854, the USDA National Institute of Food and Agriculture, AFRI project # 2018-07406, and the USDA-NIFA Hatch Project #1008750.

REFERENCES CITED

Alzagameem, A., Bergrath, J., Rumpf, J., and Schulze, M. (2022). "Lignin-based composites for packaging applications," in: *Micro and Nanolignin in Aqueous*

Dispersions and Polymers, D. Puglia, C. Santulli, and F. Sarasini (Eds.), Elsevier, pp. 131-171. DOI: 10.1016/B978-0-12-823702-1.00013-X

Duval, A., Molina-Boisseau, S., and Chirat, C. (2013). "Comparison of kraft lignin and lignosulfonates addition to wheat gluten-based materials: Mechanical and thermal properties," *Industrial Crops and Products* 49, 66-74. DOI: 10.1016/j.indcrop.2013.04.027

Ganawatta, M., Lokupitiya, H., and Tang, C. (2019). "Lignin biopolymers in the age of controlled polymerization," *NCBI*, Retrieved from https://www.ncbi.nlm.nih.gov/pmc/articles/PMC6680560/ DOI: 10.3390/polym11071176

Huang, J. (2019). "Structure and characteristics of lignin," in: *Lignin Chemistry and Applications*, J. Huang, S. Fu, and L. Gan (Eds.), Elsevier, City, Country, pp. 25-50. DOI: 10.1016/B978-0-12-813941-7.00002-3

Jokinen, V., Sainiemi, L., and Franssila, S. (2011). "Controlled lateral spreading and pinning of oil droplets based on topography and chemical patterning," *Langmuir* 27(11), 7314-7320. DOI:10.1021/la200511q

Laurichesse, S., and Avérous, L. (2014). "Chemical modification of lignins: Towards biobased polymers," *Progress in Polymer Science* 39(7), 1266-1290. DOI: 10.1016/j.progpolymsci.2013.11.004

Liu, X., Wang, J., Li, S., Zhuang, X., Xu, Y., Wang, C., and Chu, F. (2014). "Preparation and properties of UV-absorbent lignin graft copolymer films from lignocellulosic butanol residue," *Industrial Crops and Products* 52, 633-641. DOI: 10.1016/j.indcrop.2013.11.036

Livi, S., Bugatti, V., Marechal, M., Soares, B. G., Barra, G. M. O., Duchet-Rumeau, J., and Gérard, J.-F. (2015). "Ionic liquids–lignin combination: an innovative way to improve mechanical behaviour and water vapour permeability of eco-designed biodegradable polymer blends," *RSC Advances* 5(3), 1989-1998. DOI: 10.1039/C4RA11919C

Lu, F., and Ralph, J. (2010). "Lignin," in: *Cereal Straw as a Resource for Sustainable Biomaterials and Biofuels*, R.-C. Sun (ed.), Elsevier, Amsterdam, Ch. 6, pp. 169-207. DOI: 10.1016/B978-0-444-53234-3.00006-7

Menossi, M., Cisneros, M., Alvarez, V. A., and Casalongué, C. (2021). "Current and emerging biodegradable mulch films based on polysaccharide bio-composites. A review," *Agronomy for Sustainable Development* 41(4), article 53. DOI: 10.1007/s13593-021-00685-0

Santos, A., Furuyama, A., Tiera, M., and Oliviera, V. (2019). "Biopolymeric films of amphiphilic derivatives of chitosan: A physicochemical characterization and antifungal study," *NCBI*, Retrieved from (https://www.ncbi.nlm.nih.gov/pmc/articles/PMC6747211/).

Shankar, S., Reddy, J. P., and Rhim, J.-W. (2015). "Effect of lignin on water vapor barrier, mechanical, and structural properties of agar/lignin composite films," *International Journal of Biological Macromolecules* 81, 267-273. DOI: 10.1016/j.ijbiomac.2015.08.015

Vásquez-Garay, F., Carrillo-Varela, I., Vidal, C., Reyes-Contreras, P., Faccini, M., and Teixeira Mendonça, R. (2021). "A review on the lignin biopolymer and its integration in the elaboration of sustainable materials," *Sustainability* 13(5), article 2697. DOI: 10.3390/su13052697

Wang, Y., Deng, C., Cota-Ruiz, K., Peralta-Videa, J. R., Sun, Y., Rawat, S., Tan, W., Reyes, A., Hernandez-Viezcas, A., Niu, G., *et al.* (2020). "Improvement of nutrient elements and allicin content in green onion (*Allium fistulosum*) plants exposed to CuO nanoparticles," *Science of The Total Environment* 725, article ID 138387. DOI: 10.1016/j.scitotenv.2020.138387

Wenzel, R. N. (1936). "Resistance of solid surfaces to wetting by water," *Industrial & Engineering Chemistry* 28(8), 988-994. DOI:10.1021/ie50320a024

Zadeh, E. M., O'Keefe, S. F., and Kim, Y.-T. (2018). "Utilization of lignin in biopolymeric packaging films," *ACS Omega* 3(7), 7388-7398. DOI: 10.1021/acsomega.7b01341

Article submitted: March 28, 2023; Peer review completed: May 6, 2023; Revised version received and accepted: July 5, 2023; Published: July 17, 2023.
DOI: 10.15376/biores.18.3.5887-5907

APPENDIX: SUPPLEMENTARY MATERIAL

Grafting Process

The grafting process of poly(lactic-co-glycolic) acid (PLGA) on lignin (LN) to form LN-g-PLGA polymer was achieved via an acylation reaction. An amount of 4 g of PLGA was placed in a three-neck bottom flask and dissolved in 100 mL of dichloromethane (DCM) at room temperature. When the PLGA was fully dissolved, 100 µL of oxalyl chloride was added dropwise with a glass syringe and 4 mL of dimethylformamide (DMF) were added as a catalyst. The mixture was stirred for 5 hours to synthesize PLGA-Cl. The PLGA-Cl was concentrated in a Buchi R-300 rotavapor (Buchi Corporation, New Castle, DE). Next, 30 mL of dimethyl sulfoxide (DMSO) containing LN were added to the PLGA-Cl solution. The amount of LN dissolved in the 30 mL of DMSO was 1 or 0.67 g for the 1:4 and 1:6 w/w LN:PLGA ratios respectively. The LN and PLGA-Cl solution were mixed overnight under nitrogen flow. The LN-g-PLGA polymer was precipitated in 200 mL of ethyl ether and washed three times in ethyl ether to remove the remaining DMSO from the polymer. The LN-g-PLGA polymer was dissolved in 40 mL of DCM and washed with water in a decantation flask three times to remove traces of unreacted LN. The LN-g-PLGA polymer was concentrated in a rotavapor Buchi R-300 (Buchi Corporation, New Castle, DE) and freeze dried using Labconco Free zone 2.5 plus (Labconco, Kansas City, MO).

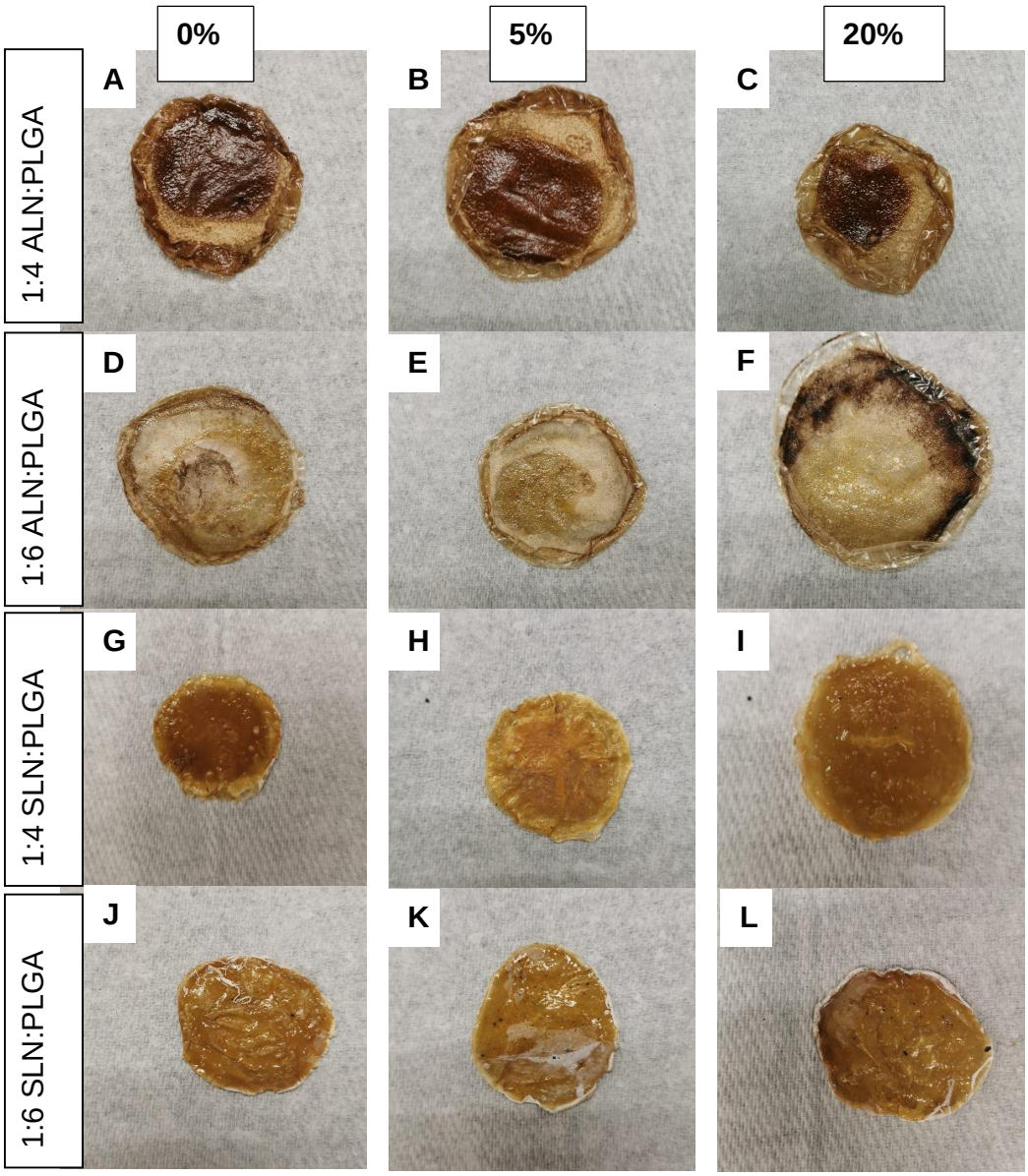

Fig. S1. LN:PLGA polymer films (A) ALN:PLGA (1:4 w/w) 0%glycerol, (B) ALN:PLGA (1:4 w/w) 5% glycerol, (C) ALN:PLGA (1:4 w/w) 20% glycerol, (D) ALN:PLGA (1:6 w/w) 0% glycerol, (E) ALN:PLGA (1:6 w/w) 5% glycerol, (F) ALN:PLGA (1:6 w/w) 20% glycerol, (G) SLN:PLGA (1:4 w/w) 0% glycerol, (H) SLN:PLGA (1:4 w/w) 5% glycerol, (I) SLN:PLGA (1:4 w/w) 20% glycerol, (J) SLN:PLGA (1:6 w/w) 0% glycerol, (K) SLN:PLGA (1:6 w/w) 5% glycerol, and (L) SLN:PLGA (1:6 w/w) 20% glycerol.

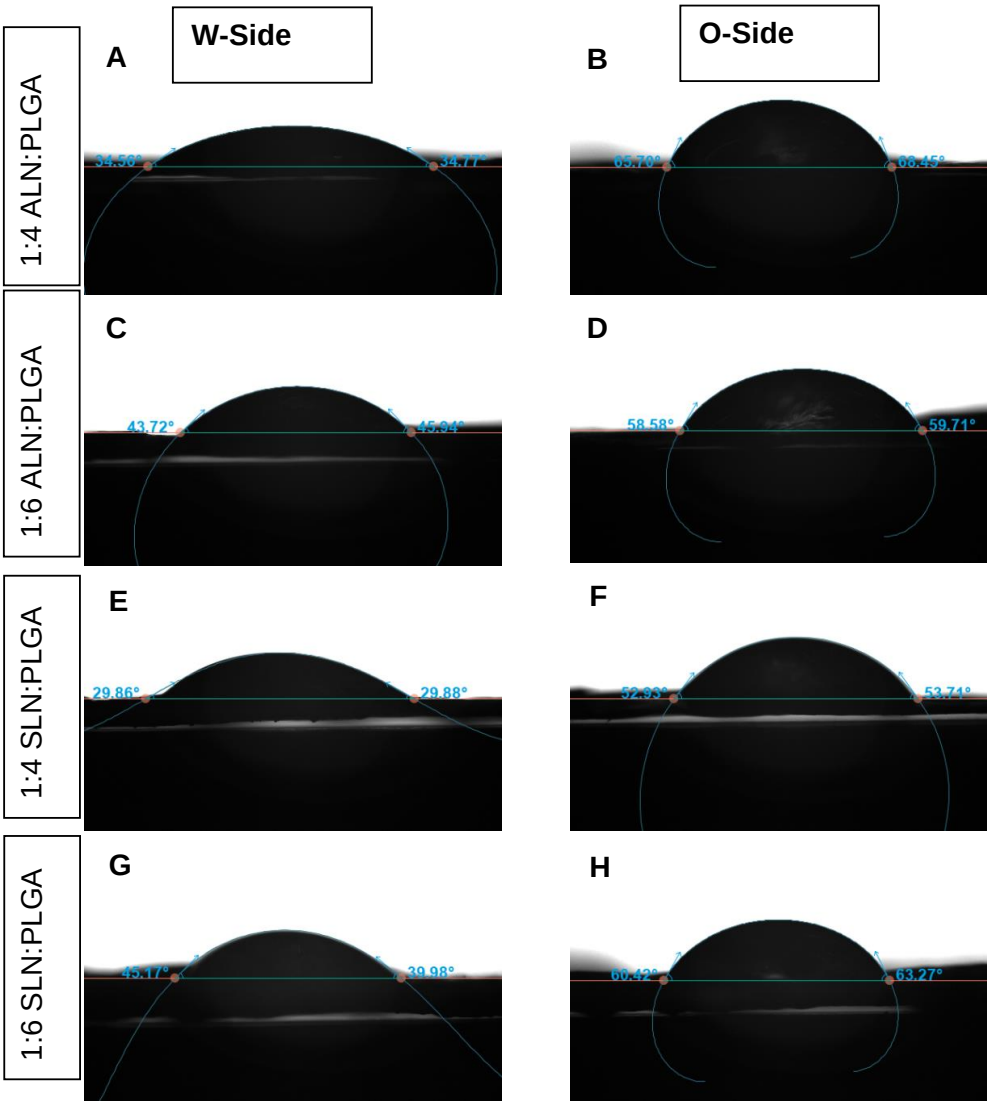

Fig. S2. Water (W) and Organic (O) side of contact angle images of (A/S)LN-g-PLGA films at different LN:PLGA w/w ratios. (A) ALN:PLGA (1:4 w/w) W side, (B) ALN:PLGA (1:4 w/w) S side, (C) ALN:PLGA (1:6 w/w) W side, (D) ALN:PLGA (1:6 w/w) O side, (E) SLN:PLGA (1:4 w/w) W side, (F) SLN:PLGA (1:4 w/w) O side, (G) SLN:PLGA (1:6 w/w) W side, (H) SLN:PLGA (1:6 w/w) O side

The average contact angle measured by the tensiometer for films with 0 % glycerol were the following, PLGA (W = 71.8 ± 11°, O = 70 ± 7.2°), ALN 1:4 w/w (W = 27.2 ± 7.2°, O = 59.7 ± 12.8°), ALN 1:6 w/w (W = 42 ± 8.5°, O = 65.3 ± 6.1°), SLN 1:4 w/w (W = 50 ± 12.1°, O = 54.8 ± 19.6°), and SLN 1:6 w/w (W = 63.3° ± 12.9, S = 63.4° ± 10) .

Contact angle can be different depending on the roughness of the surfaces. The direct relation between the hydrophobicity and the chemical makeup of material is explained by the intrinsic contact angle, that corresponds to the contact angle that a liquid would make in an ideal flat surface. Nevertheless, because most surfaces are not completely

flat, Wenzel equation is used to determine the interaction between hydrophobicity and roughness of a surface.

$$cos\theta_w = \bar{r} \cos \theta_y \quad (1)$$

In Eq. 1, θ_w corresponds to the apparent contact angle that can be measured using an optical tensiometer, $\bar{r}$ refers to the roughness coefficient of the surface, and θ_y equals the intrinsic contact angle. This equation shows a correlation within the roughness and the contact angle. Roughness increases the effect of the intrinsic hydrophobicity of the material. With higher roughness the surface area between the solid and liquid phases increases and hydrophilic surface would become more hydrophilic and vice versa for hydrophobic surfaces (Wenzel 1936). This would match up with observed results, as R sides of the films were not strictly hydrophobic but the roughness of this side of the films enhanced their hydrophobicity. The W-sides had a lower contact angles compared to the O-side of the films, which were more hydrophilic. A contact angle above 90° is specific to hydrophobic surfaces, while a surface with a contact angle higher than 90° is considered hydrophilic (Jokinen *et al*. 2011).

Table S1. Analysis of Variances for Chemical Composition on LN-g-PLGA Films with Three Variables: Side, Lignin type, LN:PLGA Ratio. " * " P≤0.05, " ** " P≤0.005, and "***" P≤0.0005. n=3

Variable	Carbon (%)[a]	Sulfur (%)[a]	C-C/C-H (Alkanes) (%)[b]	C-O-C/C-OH (Ether/Hydroxyl) (%)[b]	O-C=O (Ester) (%)[b]
Side	P=0.0356 *	P=0.0002 ***	P=0.1164 ns	P=0.0121*	P=0.0011**
Lignin type	P=0.5405 ns	P=0.0582 ns	P=0.0045 **	P=0.6849 ns	P<0.0001***
Ratio	P=0.0845 ns	P=0.0462 *	P=0.4731 ns	P=0.5719 ns	P=0.4308 ns
Side x Lignin type	P=0.0077 **	P=0.0279 *	P=0.2959 ns	P=0.0551 ns	P=0.0374 *
Side x Ratio	P=0.8175 ns	P=0.2970 ns	P=0.1087 ns	P=0.5992 ns	P=0.0036 **
Lignin type x Ratio	P=0.1416 ns	P=0.1624 ns	P=0.7711 ns	P=0.2224 ns	P=0.0062 **
Side x Lignin type x Ratio	P=0.3698 ns	P=0.3738 ns	P=0.0102 *	P=0.0719 ns	P=0.0102 *

[a]Carbon and sulfur concentrations

[b]Carbon bond analysis amounting to 100 % carbon content.

Table S2. Analysis of Variances for Contact Angle on the W- and O- Sides of LN-g-PLGA Films with Three Variables: Glycerol, Lignin type, and LN:PLGA Ratio. " * " P≤0.05, " ** " P≤0.005, and "***" P≤0.0005. n=3.

Variable	Water-side	Oil-side
Glycerol	P=0.2331 ns	P=0.2420 ns
Lignin type	P=0.0004 ***	P=0.1883 ns
Ratio	P=0.0006 ***	P=0.2934 ns
Glycerol x Lignin type	P=0.2175 ns	P=0.8123 ns
Glycerol x Ratio	P=0.6499 ns	P=0.0898 ns
Lignin type x Ratio	P=0.3425 ns	P=0.3569 ns
Glycerol x Lignin type x Ratio	P=0.3181 ns	P=0.5810 ns

Table S3. Analysis of Variances for Contact Angle on LN-g-PLGA Films at Three Glycerol Concentrations (%) with Three Variables. Side, Lignin Type, and LN:PLGA Ratio. " * " P≤0.05, " ** " P≤0.005, and "***" P≤0.0005. n=3.

Variable	0% glycerol	5% glycerol	20% glycerol
Side	P=0.0014 **	P<0.0001 ****	P<0.0001 ****
Lignin type	P=0.0390 *	P=0.1916 ns	P=0.9878 ns
Ratio	P=0.0202 *	P=0.0364 *	P=0.1236 ns
Side x Lignin type	P=0.0060 **	P=0.0794 ns	P=0.0539 ns
Side x Ratio	P=0.4273 ns	P=0.9960 ns	P=0.0016 **
Lignin type x Ratio	P=0.9267 ns	P=0.0735 ns	P=0.4950 ns
Side x Lignin type x Ratio	P=0.7980 ns	P=0.3821 ns	P=0.2698 ns

Table S4. Tukey's Multiple Comparison Test for Shrinking (%) on LN-g-PLGA." * "P≤0.05, " ** "P≤0.005, and"***"P≤0.0005. n=3

Comparison	Adjusted P-value	Classification
PLGA vs ALN 1:4	P=0.7615 ns	B vs B
PLGA vs ALN 1:6	P=0.9890 ns	B vs B
PLGA vs SLN 1:4	P=0.0023 **	B vs A
PLGA vs SLN 1:6	P=0.0059 **	B vs A
ALN 1:4 vs ALN 1:6	P=0.9476 ns	B vs B
ALN 1:4 vs SLN 1:4	P=0.0005 ***	B vs A
ALN 1:4 vs SLN 1:6	P=0.0011 **	B vs A
ALN 1:6 vs SLN 1:4	P=0.0012 **	B vs A
ALN 1:6 vs SLN 1:6	P=0.0030 **	B vs A
SLN 1:4 vs SLN 1:6	P=0.9599 ns	A vs A

Table S5. Analysis of Variances for Thickness (µm) on LN-g-PLGA Films with Three Variables: Glycerol, Lignin Type, and LN:PLGA Ratio. " * " P≤0.05, " ** "

Variable	P-value
Glycerol	P=0.1482 ns
Lignin type	P=0.0510 ns
Ratio	P=0.0053 **
Glycerol x Lignin type	P=0.1826 ns
Glycerol x Ratio	P=0.1050 ns
Lignin type x Ratio	P=0.5597 ns
Glycerol x Lignin type x Ratio	P=0.0009 ***

P≤0.005, and "***" P≤0.0005. n=3

Table S6. Analysis of Variances for Mechanical Properties on LN-g-PLGA Films with Three Variables: Side, Lignin Type, LN:PLGA Ratio. " * " P≤0.05, " ** "

Variable	Maximum strength (MPa)	Elastic limit strength (MPa)	Strength at break point (MPa)	Young modulus (GPa)	Strain at break point (%)
Glycerol	P=0.1838 ns	P=0.5132 ns	P=0.363 ns	P=0.7186 ns	P=0.4260 ns
Lignin type	P<0.0001 ***	P<0.0001 ***	P<0.0001 ***	P<0.0001 ***	P<0.0001 ***
Ratio	P=0.6284 ns	P=0.2649 ns	P=0.1224 ns	P=0.0116 *	P=0.1816 ns

P≤0.005, and "***" P≤0.0005. n=3